# Direct observations of field-induced assemblies in magnetite ferrofluids

N. S. Susan Mousavi, Sachin D. Khapli, and Sunil Kumar

Citation: Journal of Applied Physics **117**, 103907 (2015); doi: 10.1063/1.4914484
View online: http://dx.doi.org/10.1063/1.4914484
View Table of Contents: http://scitation.aip.org/content/aip/journal/jap/117/10?ver=pdfcov
Published by the AIP Publishing

# Direct observations of field-induced assemblies in magnetite ferrofluids

N. S. Susan Mousavi,[1] Sachin D. Khapli,[2] and Sunil Kumar[1,2]
[1]*Mechanical Engineering Department, Polytechnic School of Engineering, New York University, 6 Metrotech Center, Brooklyn, New York 11201, USA*
[2]*New York University Abu Dhabi, Saadiyat Island, PO Box 129 188, Abu Dhabi, United Arab Emirates*

(Received 15 September 2014; accepted 28 February 2015; published online 11 March 2015)

Evolution of microstructures in magnetite-based ferrofluids with weak dipolar moments (particle size $\leq 10$ nm) is studied with an emphasis on examining the effects of particle concentration ($\phi$) and magnetic field strength ($H$) on the structures. Nanoparticles are dispersed in water at three different concentrations, $\phi = 0.15\%$, 0.48%, and 0.59% ($w/v$) [g/ml%] and exposed to uniform magnetic fields in the range of $H = 0.05$–0.42 T. Cryogenic transmission electron microscopy is employed to provide *in-situ* observations of the field-induced assemblies in such systems. As the magnetic field increases, the Brownian colloids are observed to form randomly distributed chains aligned in the field direction, followed by head-to-tail chain aggregation and then lateral aggregation of chains termed as zippering. By increasing the field in low concentration samples, the number of chains increases, though their length does not change dramatically. Increasing concentration increases the length of the linear particle assemblies in the presence of a fixed external magnetic field. Thickening of the chains due to zippering is observed at relatively high fields. Through a systematic variation of concentration and magnetic field strength, this study shows that both magnetic field strength and change in concentration can strongly influence formation of microstructures even in weak dipolar systems. Additionally, the results of two commonly used support films on electron microscopy grids, continuous carbon and holey carbon films, are compared. Holey carbon film allows us to create local regions of high concentrations that further assist the development of field-induced assemblies. The experimental observations provide a validation of the zippering effect and can be utilized in the development of models for thermophysical properties such as thermal conductivity. © *2015 AIP Publishing LLC*.
[http://dx.doi.org/10.1063/1.4914484]

## I. INTRODUCTION

Ferrofluids are colloidal dispersions of single domain ferri-or ferro-magnetic nanoparticles (generally with the size $\leq 10$ nm) dispersed in a carrier liquid and stabilized by a coating of surfactant. A useful feature of ferrofluids is that the physical properties such as thermal conductivity and viscosity could be modulated by the application of external magnetic field (MF) while retaining the fluidic nature of the dispersions. In the absence of an external field, magnetic moments of the individual nanoparticles are randomly oriented and show no long-range order. However, dipolar moments tend to align with the field direction when a ferrofluid is exposed to a magnetic field.[1–4]

Interactions between magnetic nanoparticles when coupled to the applied magnetic field lead to field-induced assemblies, respectively, of the particles into 1D, 2D, or 3D aggregates; from dipolar flexible chains[5,6] to other heterogeneous structures aligned along the field.[7] Formation of these structures, in particular, ordered chains or columnar structures in ferrofluids as a result of an applied field, leads to a change in the macroscopic properties of the medium,[8,9] while thermodynamic properties such as effective heat capacity remain unaffected by these heterogeneous structures.[10] For instance, magnetization of ferrofluid increases with the growth of chains,[2,11–14] viscosity abruptly increases,[1,2,15] thermal conductivity is enhanced if the field direction is parallel to temperature gradient,[16–20] and optical properties become strongly anisotropic.[1,21–23]

There are several examples of successful and prospective applications of self-assembled or field-assisted magnetic nanoparticles from technical applications to medical ones: in data storage, electronic devices, sensors, rotating shaft seals, hydrostatic and hydrodynamic bearings, magnetoacoustic transducers, vibration isolation and inertia damping systems, thermal systems, medical diagnostics, therapy and drug delivery, biophysical studies, and magnetic biosensing.[24–31] In order to engineer field-induced structures[25,32,33] in ferrofluids, it is necessary to understand the interactions between the magnetic particles and the parameters by which the structure formation can be controlled. Our work is motivated by the ability to control heat transport in ferrofluids by the application of magnetic fields[8,34] and the development of the models for thermophysical properties.

For such applications, superparamagnetic particles with weak dipolar interactions at room temperature are favorable because the smaller particle size (1–10 nm) ensures stability of the dispersion against sedimentation in gravitational field as well as magnetic agglomeration in zero field.[1,35]

Weak dipolar interactions ensures reversibility of the field-assisted assembly processes upon removal of the field as thermal energy is capable of overcoming weak dipolar interactions resulting in redistribution of the particles homogeneously throughout the medium.

 

Evolution of such ferrofluids structures has been studied both theoretically and experimentally. A number of theoretical models have been used in numerical simulations, for instance, Monte Carlo (MC) or Brownian dynamics method.[1,36–40] A variety of experimental techniques has been used in order to observe formation of structures. Amongst these techniques are SEM (Scanning Electron Microscopy), TEM (Transmission Electron Microscopy) and Cryo-TEM (Cryogenic Electron Microscopy), Optical Microscopy, small-angle neutron scattering (SANS),[41] light scattering and scattering dichroism, Raman spectroscopy,[42] and X-ray scattering (SAXS),[2,3,27,45–47] each with its advantages and disadvantages. For instance, it is argued that TEM method may not give an accurate feature of the evolution of dipolar structures in liquid phase because during evaporation of the solvent distortions and sometimes cracks are formed by surface tension. Additionally, evaporation of solvent in preparation of TEM grids causes dipolar moments to become gradually dominant while eliminating the role of the fluid, such as the presence of Brownian motion.[6]

Cryo-TEM is suitable for *in-situ* observations of ferrofluids because it enables the imaging of particles down to 2 nm resolution. This technique was first demonstrated by Butter *et al.*[6] for the direct observation of dipolar chains in iron-based ferrofluids. They showed the formation of randomly oriented linear aggregates and branched chains or networks in zero field when the particle size was increased from $2.1 \pm 0.3$ nm to $6.9 \pm 1.0$ nm. Formation of aligned chains and thick elongated structures was also observed when the samples were vitrified in magnetic field of 1.6 T. Wu *et al.*[43] studied field-induced assemblies in 6 nm superparamagnetic magnetite ferrofluids using cryo-TEM and demonstrated the formation of short dipolar chains as well as flux-closure rings. Klokkenburg and Ern[44] used the technique in conjunction with complex magnetic susceptibility measurement to correlate the macroscopically averaged behavior with the microstructures formed in partially oxidized iron/iron oxide ferrofluids.

The formation of microstructures in weakly dipolar ferrofluids, as influenced by the concentration of nanoparticles $\phi$ and applied magnetic field $H$, has not been explored previously by the technique of cryo-TEM. In our study, these two parameters are varied systematically and qualitative explanations are provided for the cryo-TEM observations of sub 10 nm magnetite ferrofluids based on a simple mean-field thermodynamical analysis.

Further, different types of commonly used support films on the Electron Microscopy (EM) grids have been examined and the results are compared.

On a qualitative level, the set of images presented in this study will shed light on finding an optimal procedure to engineer and control field-assisted structures into desired assemblies, while benefiting from the advantages of having weak dipolar systems ensuring long term stability of the mediums upon application or removal of an external field. The present study provides not only experimental basis for developing models for thermal conductivity and other thermophysical properties but also experimental evidence for the zippering transitions in weakly dipolar ferrofluids under applied magnetic field.

## II. MATERIALS AND METHODS

Surfacted magnetite particles dispersed in water were chosen. According to TEM images, the size of magnetic nanoparticles including steric layer is $\leq$10 nm for at least 90% of nanoparticles. The polymer shell of the particle is sodium polyacrylic acid derivative (<1% by weight). Suspensions and magnetite powder were purchased from *Vivenano* and *Sciventions*. The samples with different concentrations (whose characteristics can be found in Table I) were prepared either by adding water to or by evaporating water and adding magnetite powder to the original samples. The samples of concentration 0.48% labeled B-1 and B-2 (see Table I) were, respectively, made by concentrating the original sample of 0.15% purchased from *Vivenano* and by diluting the original sample of 0.59% purchased from *Sciventions*.

Magnetic nanoparticles are coated by surfactant to ensure long term stability of the ferrofluid. The adsorbed polymer, sodium polyacrylate, is negatively charged at basic pH and provides better stabilization. Although the samples were found to be stable for months, the pH of the samples was measured before every experiment. After dilution and addition of magnetic powder, if the pH was found below 10, it was adjusted by addition of NaOH solution. Additionally, a probe sonicator was used for approximately 2 min or, in case of bath sonicator, the samples were placed in the sonicator for 10 min. Since power levels are lower for bath sonicators, it requires more time for dispersion.

Prior to plunging, grids were cleaned in a Hydrogen/Oxygen plasma using Gatan Solarus 950 plasma cleaner. The plasma cleaner was operated at 50 W RF power for 20 s to remove hydrocarbon impurities from the surface by treatment with glow-discharge plasma and render the surface hydrophilic. For cryo-TEM samples, two different types of 300 mesh grids, continuous carbon coated copper grids (CF300-Cu) and holey carbon film on copper grid (Quantifoil R2/2-Cu) purchased from Electron Microscopy Sciences and SPI supplies, respectively, were used. Grids in magnetic field were plunged using a custom made manual plunger. A homogenous and constant magnetic field was generated using four axially magnetized neodymium cylindrical magnets N42-DEX2 (K&J magnetic, Inc.) with the help of a custom built setup. The setup holds magnets and allows the distance between poles of the magnets to be changed in order to generate an adjustable external magnetic field.

TABLE I. Characteristics of superparamagnetic magnetite aqueous samples: particle diameter (nm) according to TEM, and sample concentration ($\phi$) *w/v*% [g/ml%].[a]

| Code | A | B-1 | B-2 | C |
|---|---|---|---|---|
| $d_{TEM}$ | 1–10 | 1–10 | 1–10 | 1–10 |
| *Concentration* | 0.15 | 0.48 | 0.48 | 0.59 |

[a]Particle concentration $\phi$ is related to particle volume fraction $\varphi$ as $\phi = \rho\varphi$, where $\rho$ (density of bulk magnetite) = 5.24 (g/cm$^3$).

Both the plunger and the magnet holder stand were placed in a humidity and temperature controlled chamber while making cryo-TEM samples. After cleaning a grid, it was then placed parallel to the magnetic field and 4 $\mu$l of a sample was applied onto it. In preparing the grids, no-blotting method was employed to keep the particles arrangements untouched. The grid was instead left in magnetic field for approximately 20 min in order to drain excessive water from the sample, also allowing the microstructures to be steadily formed. Light scattering studies show that this is enough time to reach stable state before cryo-freezing is initiated.[42] Then, the grid was immediately plunged into liquid ethane.

The vitrified samples were stored in storage tanks of liquid nitrogen. The grid was loaded onto a Gatan 626 cryo-holder and was later transferred to JEOL 2100, 200 kV microscope, or TECNAI F20 200 kV for imaging. Images were taken at low dose condition while varying magnification. For cryo-TEM grids in zero field, the automatic plunger Gatan CP3 was used, but for vitrification of the grids, the same procedure as using a manual plunger was followed.

## III. RESULTS AND DISCUSSION

A series of cryo-TEM images were taken under low dose conditions from TEM grids that were vitrified in magnetic field. Magnetic field was introduced by placing the grids in between rare-earth magnets of known magnetization. As the grids are much smaller than the distance over which magnetic field is applied between the rare-earth magnets, the applied field can be assumed to be uniform across the TEM grids.[8]

As the single domain crystalline iron oxide particles noticeably enhance image contrast as compared to both the carrier liquid, i.e., water, and ice crystals, magnetic particles structures can be easily visualized. Ice crystals seen on some of the electron micrographs were found to have no effect on the morphology of the magnetic particles assemblies.

Cryo-TEM imaging was performed under zero-field as well as in-field conditions. Both, the field strength as well as the particle concentration were varied systematically to investigate the transition of field-induced structures from homogeneously dispersed particles mixed with dipolar short chains in zero field to other heterogeneous structures in the presence of applied field. In the following discussion, we present the results of our observations of zero-field and in-field structures, followed by the observation of columnar structures in high field and the influence of supporting films on the in-field structures.

### A. Zero-field structures

The morphology of zero field equilibrium structures has been theoretically studied and examined by many experimental observations in details.[2,5,6,11]

Dipolar energy between the two particles depends on not only magnetic moment of the particles (material properties, particle size or taking into account size distribution of the particles, i.e., polydispersity) but also distances between the particles (concentration $\phi$). It was shown[25] that for given superparamagnetic particles (known size and material) in the absence of a magnetic field, dipolar energy is strongly distance dependant; in small separations it scales with $r^{-3}$ whereas for larger separations it decays with $r^{-6}$, where $r$ is the distance between the particles.[1] The dipole-dipole energy is characterized by the magnitude of the energy when the two particles are in contact, that is $(m^2/16\pi\mu_0 a^3)$. Coupling constant coefficient, $\lambda = (m^2/32\pi\mu_0 a^3 k_B T)$, is a dimensionless parameter that gives a measure of dipolar contact energy in comparison to thermal energy $k_B T$.[1] $m$, $\mu_0$, $a$, $k_B$, and $T$ are magnetic moment of particles, permeability of free space, particle's radius, Boltzmann's constant, and temperature, respectively. Magnetic moment of a particle is $m = \mu_0 M_d V_p$, where $M_d$ and $V_p$ are, respectively, domain magnetization and volume of a particle.

Without an external field when $\lambda > 1$, equivalently when the characteristic dipole energy exceeds $2k_B T$, self-assembly of particles is expected. In a surfactant-stabilized ferrofluid with small $\lambda$, thermal energy balances the weak dipolar interactions, thus the medium can be treated as a homogenous colloid whose particles are dispersed spatially random in the liquid.[2,3] If steric layer is taken into account physically relevant quantity is $\lambda^* = (d_m/d_h)^3 \lambda$, where $d_m$ is the magnetic core diameter and $d_h$ is diameter of particle including steric layer.[2] For a typical ferrofluid, steric layer is about 2–4 nm that gives a smaller value for $\lambda^*$ than $\lambda$ by a factor of 2–3.

If $\lambda \gg 1$ because of magnetic particles with larger bulk saturation magnetization, or having lager particles, or having a low temperature, thermal energy is not capable of overcoming dipolar interactions, therefore the fluid develops microstructures in zero field such as a pair of particles, rings, worm-like short chains, and flux closure rings.

Mean number of particles in the chain at zero field can be theoretically calculated as $n_0 = [1 - \frac{2}{3}(\varphi/\lambda^3)e^{2\lambda}]^{-1}$, where $\varphi$ is volume fraction of particles.[1]

In a weak dipolar system of magnetite ($Fe_3O_4$) based ferrofluid, with particles of 10 nm in size (a = 5 nm), $M_d = 446$ (kA/m) in contact, and $\varphi = 0.05$, $n_0$ equals to 1.26 at room temperature which implies for dilute suspensions of monodisperse magnetite particles with size <10 nm, a little clustering or agglomeration is expected.[1] The magnitude of characteristic dipolar interaction energy for this system is $2.63 k_B T$ that is not strong enough to induce development of zero-field self-assembled structures.

Cryo-TEM image of zero-field sample verifies random dispersion of particles mixed with some aggregates (see page 19, Ref. 8).

### B. Field-induced structures

Morphologies of the field-assisted structures have been studied theoretically and experimentally.[2,3,11,36–39,45,48]

There are many factors that influence the morphologies of field-induced microstructures such as dipolar strength, magnetic field orientation and strength, thickness of the sample, polydispersity, concentration of the particles, and temperature. In a qualitative view, the morphology of the structures depends on particle-particle interactions characterized by $\lambda$, as well as particle-field interactions characterized

by $\alpha$ where $\alpha = mH/k_BT$, known as energy ratio or Langevin parameter and $H$ is magnetic field strength. In practice, when the characteristic dipole energy falls within the range of $\sim 2k_BT$ to $\sim 8k_BT$, the structures can be assembled and disassembled through the application or removal of an external field, although the interactions are still weak to induce self-assembled structures.[25]

When a magnetic field is in place, polarization of the ferrofluid takes place and fluctuating dipole moments of individual nanoparticles get aligned in the field direction. The particle-field interactions become strong enough to overcome the thermal energy when $\alpha > 1$. Under such conditions, the dipole-dipole interactions are also intensified due to preferential alignments of the individual dipoles, resulting in the formation of field-induced structures such as chains and columns.

Both concentration and coupling to the magnetic field are responsible for the transition from dipolar short chains to columnar ordering, and to the thick bundles both of which are discussed in the two separate sections. The columnar structures and the comparison between the two types of the grids will also be addressed subsequently.

#### 1. Effects of concentration in a known magnetic field

For a ferrofluid with low concentration, the two parameters, concentration and coupling constant coefficient, can be combined into the Langevin initial susceptibility $\chi_i = 8\varphi\lambda$. For weakly dipolar systems (small $\lambda$), the initial susceptibility increases linearly with the particle volume fraction $(\varphi)$. In a given ferrofluid with weak dipolar interactions, the development of field-assisted structures by varying concentration can be related to the dependency of the initial susceptibility on concentration.

Increasing concentration results in increasing initial susceptibility and saturation magnetization of the sample due to the formation and development of microstructures.[14] The process can be described that higher concentration hinders both the thermal diffusion of the particles and intensify particle-particle interactions, because there will be less accessible sites for the particles to move freely. Also, it brings the particles close enough to each other giving them an opportunity to interact with their magnetic moments.

Higher concentration in this scenario simply means there exist greater fraction of short dipolar chains. As mentioned earlier, one trend in field-induced assemblies is the alignment of the previously formed zero-field structures in magnetic field. Therefore, the switch to longer chains will occur with increase in concentration which was demonstrated in simulation as well.[38] Also, in an appropriately high concentration chains become thicker as they adsorb neighboring structures. In an agreement with simulation,[39] thicker chains are seen in higher concentrations though the field strength is the same (follow the trend in the insets of Fig. 1 at each row, from left to right). The insets on the top row in Fig. 1, show increase in concentration from the left to the right in a relatively weak magnetic field of 515 gauss (51.5 mT). This set can be compared with the sets in second and third rows with magnetic fields of 0.2 and 0.42 T, respectively. Several longer chains can be observed in the inset 3 of Fig. 1 than in 5, and than in 7. However, the geometrical non-linearity of the chains indicates that magnetic field is not strong enough to completely align particles' moments in a head-to-tail bond and they fluctuate within the particles. These findings are similar to the results described in theory and simulations.[11]

Figure 2 demonstrates a qualitative relationship between increase in magnetization of each sample as field increases, with the growth of the chains in them. It is seen that none of the samples are saturated at the 515 gauss magnetic field strength. Therefore, chains are not perfectly straight (see the top row of Fig. 1). In the second row, the magnetic field strength is strong enough to bring the sample of 0.15% close to saturation state, while the other two samples are still showing more capacity to increase magnetization. This implies that for the sample of 0.15% increase in length of the chains is not anticipated but their geometric linearity and perhaps thickness (see Fig. 3) should increase. Whereas for the other two samples chains not only can become longer but can also become straighter or thicker. The third row of Fig. 1 shows increase in number, length, and thickness of the chains as results of increasing the concentration.

#### 2. Effects of magnetic field on a sample with known concentration

It is known that external magnetic field causes an increase in the effective attraction of dipole particles.[13] Upon applying magnetic field to a sample, dipolar moments tend to align themselves towards the field direction. As a result, short chains that are either already formed in the sample or are being formed due to the intensification of the dipolar moments in response to the magnetic field will be oriented toward the field. The chains may not be long in low concentrations, and are loose (i.e., are easier to break) and flexible (i.e., geometrically non-linear) because of fluctuation of the moments of the individual particles within the chains. The fluctuation occurs either by Brownian rotation or Neel rotation when external field is weak. The magnetic moments of the particles become co-directed with the rise in magnetic field which decreases fluctuation in the chains. Thus, the transition of linear flexible dipolar chains to rigid rod-like (head-to-tail bond) structures (see Fig. 1, columnar order insets) occurs. The flexibility of the chains corresponds to the degree of alignment of magnetic moments within the particles in the chain. Magnetic moments become completely aligned with the magnetic field as the sample approaches saturation status.

Relative position of the chains is found either staggered or parallel as predicted by simulation.[36,38] Connection of the staggered short chains forms longer linear strips, while chain-chain interaction is responsible for the formation of thicker chains. The columns appear thicker in the inset 8 of Fig. 1 compared to the inset 9 which seems to be attributed to the thickness of the film on the grid. With increasing magnetic field, more short chains become connected and adsorb neighboring small structures, and more isolated particles form dipolar chains. The tendency of short structures to

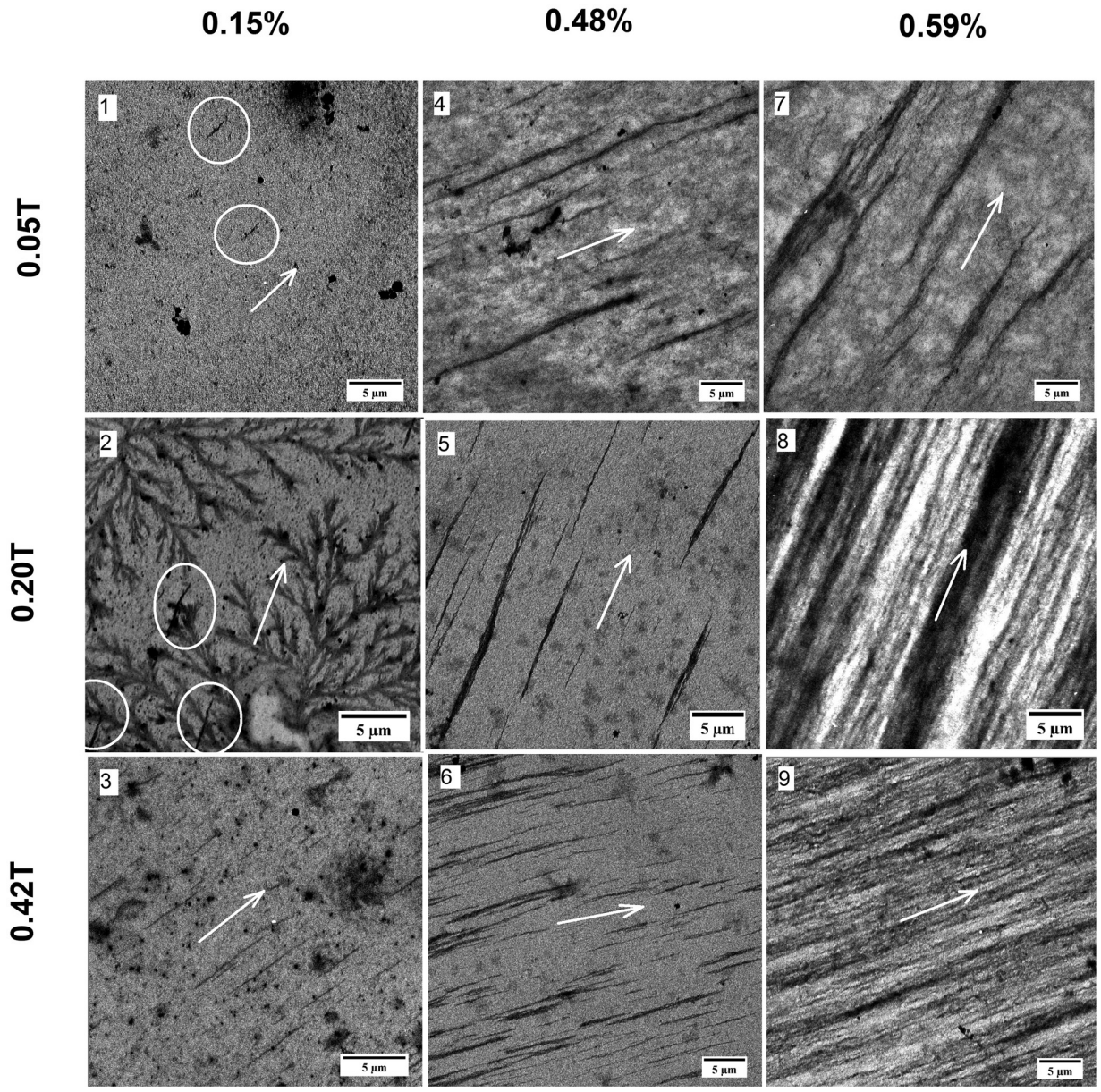


FIG. 1. Cryo-TEM images of magnetite nanoparticles in water, mean diameter of 10 nm including 2 nm thickness of coating layer (1) $\phi = 0.15\%$ ($w/v$), MF = 0.05 T; (2) $\phi = 0.15\%$ ($w/v$), MF = 0.20 T; (3) $\phi = 0.15\%$ ($w/v$), MF = 0.42 T; (4) $\phi = 0.48\%$ ($w/v$) sample B-2, MF = 0.05 T; (5) $\phi = 0.48\%$ ($w/v$) sample B-1, MF = 0.20 T; (6) $\phi = 0.48\%$ ($w/v$) sample B-1, MF = 0.42 T; (7) $\phi = 0.59\%$ ($w/v$), MF = 0.05 T; (8) $\phi = 0.59\%$ ($w/v$), MF = 0.2 T; (9) $\phi = 0.59\%$ ($w/v$), MF = 0.42 T. White arrows indicate the field direction. Circled regions indicate the microstructures. The scale bars are in 5 $\mu$m.

travel towards longer clusters due to magnetic attraction results in the growth of the strips (see Fig. 4). Lengthening of a stripe as a result of the connection between two clusters is illustrated in Fig. 5.

The growth of the small chains due to the connection of dipolar short structures decreases as the sample's magnetization approaches the saturation. Instead, the growth of the columns increases at the magnetic field strength close to the corresponding saturation value. Due to the end poles repulsion of the rigid columns, columnar structures are expected to be regularly separated.[48] To have evenly spaced columns, end pole dipole moments are important which varies with particle size. As opposed to the general theoretical assumption of neglecting polydispersity, the nanoparticle size distribution is not exactly monodisperse in practice. Therefore, the columnar distances are not uniform as predicted in theory. It is also possible that thermal fluctuations during sample preparation distort the columnar shapes, more so at low magnetic fields.

### C. Columnar structures

Once formed under the influence of an external magnetic field, the dipolar chains can undergo further aggregations processes. If the chains are aligned with their dipole moments along the same line, these interactions are always attractive and result in further increase in chain length due to head-to-tail aggregation. However, if the two chains interact with one-another in a lateral direction, these interactions can be either attractive or repulsive. When the lateral interactions cause coalescence of the chains resulting in hexagonally packed bundles, the transition is known as

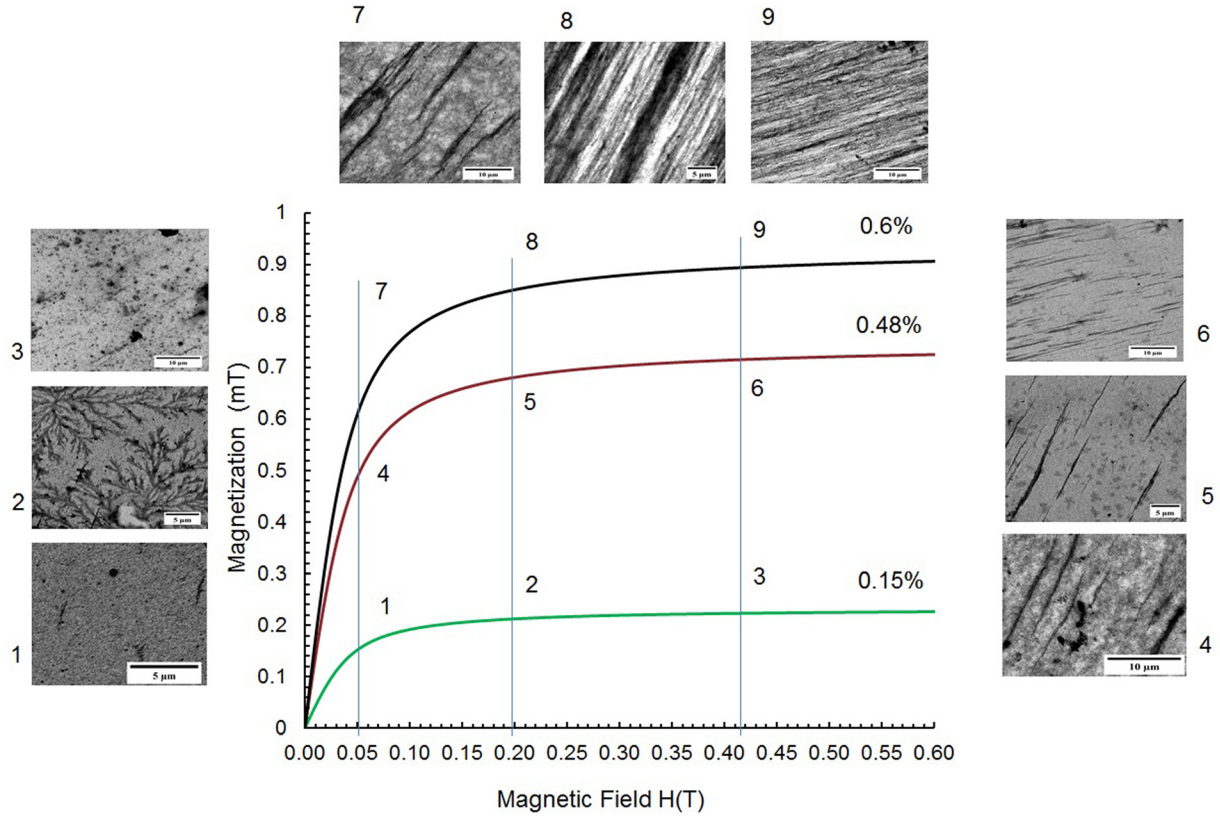


FIG. 2. Magnetization of the samples in magnetic field. Images give a qualitative demonstration of magnetization properties of each sample with the formation of chains. In low magnetic field, chains are flexible and become stiff near the saturation state.

zippering of the chains. In weakly dipolar systems, zippering occurs due to thermal-fluctuation-induced interactions between neighboring dipolar chains as explained by Martin *et al.*[49] through a modified Hasley-Toor model.[50,51] Accordingly, the lateral interaction energy per unit chain length is given by $U \sim (m/a)\langle H^2\rangle^{1/2} \sim \frac{\chi H(\mu_0 k_B T)^{1/2} a^{5/2}}{\rho^2}$, where $\rho$ is the separation between the chains.[42] Compared to the head-to-tail aggregation, the process of zippering occurs over a larger timescale and is observed only at sufficiently high field strengths where the interaction energy U, overcomes the potential energy barrier for lateral aggregation of the chains. Once formed, the zipped-superstructures are stabilized by the van der Waals interactions between the magnetic particles.[52]

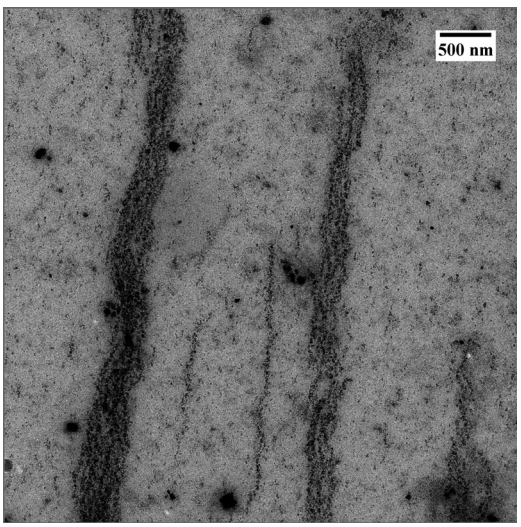


FIG. 3. Cryogenic image of the nearly saturated sample of 0.15% at 0.42 T showing thickening of the chains and variability of the thicknesses, voids can be seen within the chains.

To highlight the structure of the columns, series of images with higher magnification were taken. The insets of the image 6 give a closer look into the internal structures of the strips and columns. It also shows the existence of isolated particles and short strings in the space between columnar structures. Circular voids that were seen in simulations[39] within the columns can also be observed in the insets *b* and *c* of Fig. 6, which are attributed to the kinetically arrested defects whose relaxation requires simultaneous displacement of many neighboring dipoles.[48] Similar voids and flexibility of the chains can be seen at the end of the chains on Figs. 4 and 5. These occur where short chains come to a connection and can be explained that magnetic field is not strong enough yet to make the flexible chains rigid rod-like. It is also reported that field strengthening leads to weakening of the internal chain fluctuations which causes the chains to exhibit rigid rod-like behavior.[12]

### D. Comparison of support films

Images that were discussed in Secs. III A–III C, were taken from samples prepared on continuous carbon film on copper grid (CF300-Cu). They can be compared with the images shown in Fig. 7 taken from the vitrified samples

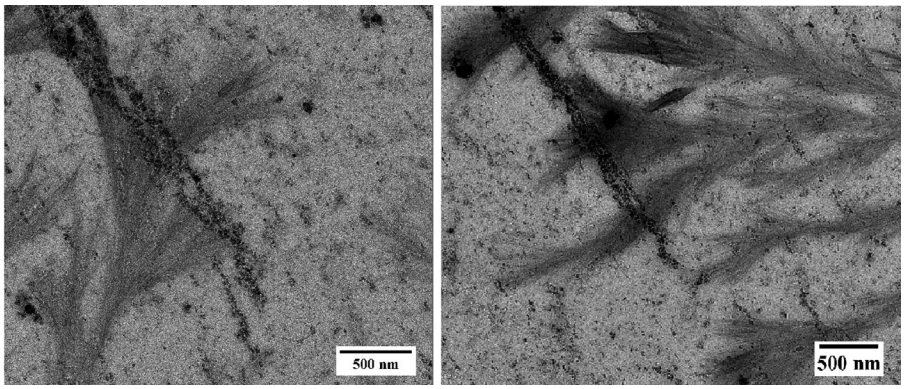


FIG. 4. Cryo-TEM images of sample of 0.15% at 0.2 T in higher magnification, showing the tendency of shorter chains to travel toward the larger structure, also the arrested void within the chains. The scale bars are in 500 nm.

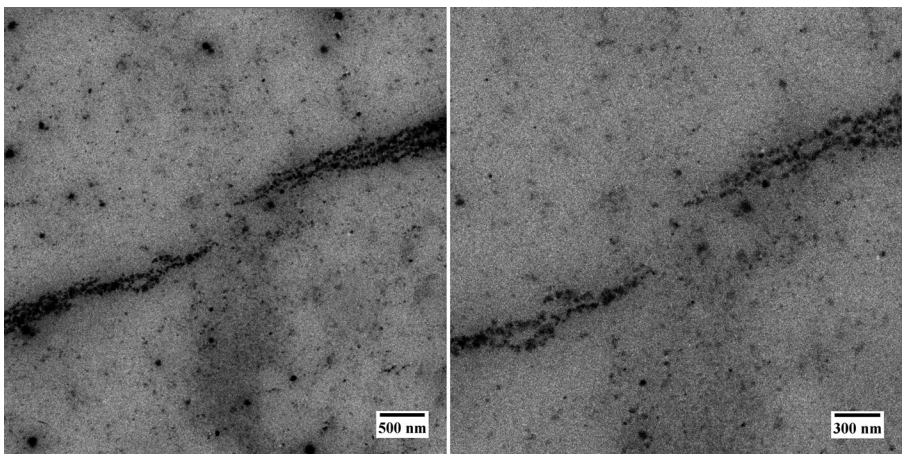


FIG. 5. Cryo-TEM images of ferrofluid of 0.15% at 0.2 T showing two elongated flexible clusters become connected, voids can be seen at the tails of the microstructures (right). The scale bars from the left to the right are in 500 nm and 300 nm, respectively.

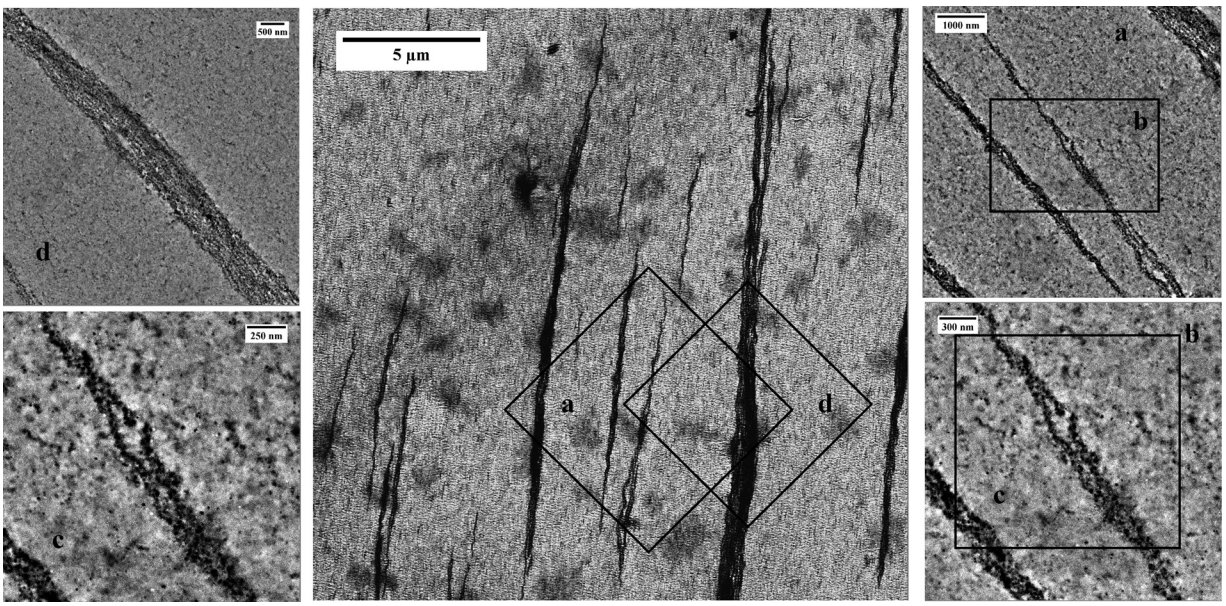


FIG. 6. Cryo-TEM images of ferrofluid 0.48% at 0.20 T magnetic field, the insets are the higher magnification images of the marked areas on the images. The scale bar in *a* is 1000 nm, in *b* is 300 nm, in *c* is 250 nm, and in *d* is 500 nm. Images were lightly processed to enhance the contrast and to reduce background noises.

prepared on holey carbon coated copper grids (Quantifoil R2/2-Cu).

The migration of magnetic particles towards the edges of the holes due to the surface tension creates locally higher concentrated regions around the holes than elsewhere on the film.[8] For the same concentration and comparable magnetic field, columnar structures are longer and straighter on holey carbon film compared to continuous carbon film. Migration of the particles around the circumferences of the holes because of the surface tension creates the regions of high-concentration in the sample. This results in increasing interaction between particles and intensifying the effect of dipolar moments, which facilitate the transition process from chains to columns. The same argument can be applied in order to

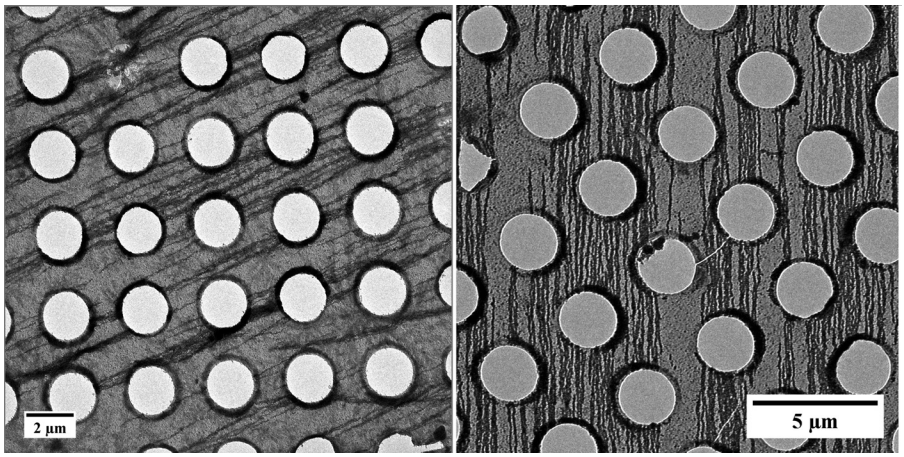


FIG. 7. Cryo-TEM images of ferrofluids (left) 0.48% at 0.2 T magnetic field showing enhancement in the formation of parallel strips because of the high-concentration regions around the holes, (right) of 0.48% ferrofluid sample nearly saturated at 0.37 T magnetic field showing enhancement in formation of elongated parallel strips on holey carbon coated grid.

describe the ordering of the particles in a relatively strong magnetic field of 0.37 T (see Fig. 7, right).

For the purpose of comparison, bare copper grids and custom made copper grids with carbon/formvar support film were also examined (see the images in Ref. 8). The bare grids did not hold the sample. The support film of carbon/formvar was found to be sensitive either to the sudden temperature change during plunge freezing or to the irradiation by electron beam. The bent coating resulted in the deformation of the microstructures.

## IV. CONCLUSIONS

Cryo-TEM observations of weakly dipolar ferrofluids are performed to investigate the effects of concentration and field strength on the nature of field-induced assemblies. As these parameters are systematically varied transitions from randomly dispersed particles to linear assemblies and zippering of the linear chains are observed.

Because of the weak dipolar interactions between the particles dipolar chains are scarce in zero field at all the concentrations studied. Increase in concentration of nanoparticles resulted in an increase in number of flexible (geometrically non-linear) chains in a weak magnetic field. In the low concentrated sample, because of the weak contact energy between particles, longer chains can be easily broken into smaller structures by thermal fluctuation. Therefore, the increment of increase of the average size of chains with magnetic field strength is small. Chains became straight and were transformed to the columnar structures in a strong magnetic field where the samples are saturated. At high magnetic field when ferrofluid is approaching the saturation point, parallel chains were lengthened across the mesh on the grid.

The columnar structures are also studied. It is observed that the tendency of the shorter structures to travel toward the larger ones at high magnetic field resulted in the lengthening of the chains. Zippering of the chains, i.e., thickening of the chains due to the lateral interactions between the staggered structures are also observed.

Through a comparison between the images of the in-field ferrofluids on two commonly used support films on EM grids: continuous carbon and holey carbon films, it was found that creation of locally concentrated regions around the holes on holey carbon film further assists development of the field-induced assemblies.

The comprehensive observation of the relatively low concentrated samples, which has not been systematically studied to the best of our knowledge, provides a qualitative basis for the field-induced assemblies under the influence of various fields and concentrations. The field-induced assemblies in weak dipolar systems could be successfully tuned by the two stimuli suggesting them as the tools that can be used in controlling and engineering the assemblies into the desired structures. The experimental observations can help in understanding the thermophysical properties of ferrofluids subjected to magnetic fields and in developing models for predicting properties such as thermal conductivity.

## ACKNOWLEDGMENTS

The data collected at the New York Structural Biology Center (NYSBC) were made possible by a grant from NYSTAR. The investigation was conducted in a facility constructed with support from Research facilities Improvement Program Grant No. C06 RR017528-01-CEM from the National Center for Research Resources, National Institutes of Health. The authors would like to thank NYSBC's staff of scientists for providing access to the cryo-TEM facilities. Special thank goes to Dr. Mariena Silvestry Ramos for her helpful advice and comments on cryogenic-TEM imaging.

[1]R. E. Rosensweig, *Ferrohydrodynamics* (Cambridge University Press, 1985).
[2]S. Odenbach, *Colloidal Magnetic Fluids* (Springer, 2009), pp. 2–30, 359.
[3]C. Holm and J. Weis, Curr. Opin. Colloid Interface Sci. **10**, 133 (2005).
[4]R. E. Rosensweig, "Ferrofluid: Introduction," in *Encyclopedia of Materials: Science and Technology* (Elsevier Science Ltd., 2001), pp. 3093–3102.
[5]M. Klokkenburg, C. Vonk, E. M. Claesson, J. D. Meeldijk, B. H. Ern, and A. P. Philipse, J. Am. Chem. Soc. **126**, 16706 (2004).
[6]K. Butter, P. H. Bomans, P. M. Frederik, G. J. Vroege, and A. P. Philipse, J. Phys.: Condens. Matter **15**, S1451 (2003).
[7]G. Bossis, L. Iskakova, V. Kostenko, and A. Zubarev, Physica A **390**, 2655 (2011).
[8]N. S. Mousavi Khoeini, "Ferrofluids: Thermophysical properties and formation of microstructures," Ph.D. dissertation (Polytechnic Institute of New York University, 2013).
[9]M. Bahiraei and M. Hangi, J. Magn. Magn. Mater. **374**, 125 (2015).
[10]N. S. Mousavi and S. Kumar, Int. J. Therm. Sci. **84**, 267 (2014).

[11]Z. Wang, C. Holm, and H. W. Müller, Phys. Rev. E: Stat., Nonlinear, Soft Matter Phys. **66**, 021405 (2002).
[12]A. Ivanov, S. Kantorovich, V. Mendelev, and E. Pyanzina, J. Magn. Magn. Mater. **300**, e206 (2006).
[13]Y. Buyevich and A. O. Ivanov, Physica A **190**, 276 (1992).
[14]M. Klokkenburg, B. H. Erné, V. Mendelev, and A. O. Ivanov, J. Phys.: Condens. Matter **20**, 204113 (2008).
[15]S. Odenbach, *Magnetoviscous Effect in Ferrofluids* (Springer, 2002).
[16]Q. Li, Y. Xuan, and J. Wang, Exp. Therm. Fluid Sci. **30**, 109 (2005).
[17]P. D. Shima and J. Philip, J. Phys. Chem. C **115**, 20097 (2011).
[18]A. Gavili, F. Zabihi, T. D. Isfahani, and J. Sabbaghzadeh, Exp. Therm. Fluid Sci. **41**, 94 (2012).
[19]C. L. Altan, A. Elkatmis, M. Yksel, N. Aslan, and S. Bucak, J. Appl. Phys. **110**, 093917 (2011).
[20]X. Fang, Y. Xuan, and Q. Li, Prog. Nat. Sci. **19**, 205 (2009).
[21]S. Brojabasi and J. Philip, J. Appl. Phys. **113**, 054902 (2013).
[22]S. Z. Malynych, A. Tokarev, S. Hudson, G. Chumanov, J. Ballato, and K. G. Kornev, J. Magn. Magn. Mater. **322**, 1894 (2010).
[23]J. J. M. Janssen and J. A. A. J. Perenboom, J. Magn. Magn. Mater. **81**, 14 (1989).
[24]S. Singamaneni, V. N. Bliznyuk, C. Binek, and E. Y. Tsymbal, J. Mater. Chem. **21**, 16819 (2011).
[25]K. J. M. Bishop, C. E. Wilmer, S. Soh, and B. A. Grzybowski, Small **5**, 1600 (2009).
[26]C. C. Wu, L. Y. Lin, L. C. Lin, H. C. Huang, Y. F. Yang, Y. B. Liu, M. C. Tsai, Y. L. Gao, W. C. Wang, S. W. Hung *et al*., Appl. Phys. Lett. **92**, 142504 (2008).
[27]R. B. Gupta and U. B. Kompella, *Nanoparticle Technology for Drug Delivery* (Taylor and Francis Group, 2006).
[28]M. Sadoqi, S. Kumar, V. Saxena, and C. Lau-Cam, *Nanotechnologies for the Lifesciences*, Biological and Pharmaceutical Nanomaterials Vol. 2, edited by C. Kumar (Wiley, 2006).
[29]V. Saxena, M. Sadoqi, S. Kumar, and J. Shao, OE Mag. - Spec. Ed. Biotechnol. **4**(9), 21–23 (2004).
[30]V. Saxena, M. Sadoqi, J. Shao, and S. Kumar, J. Biomed. Nanotechnol. **1**(2), 168–175 (2005).
[31]V. S. Kalambur, B. Han, B. E. Hammer, T. W. Shield, and J. C. Bischof, Nanotechnology **16**, 1221 (2005).
[32]D. Ortega, N. Prez, J. L. Vilas, J. S. Garitaonandia, K. Suzuki, J. R. Marn, and M. Rodrguez, J. Appl. Phys. **113**, 17B505 (2013).
[33]K. J. Mutch, V. Koutsos, and P. J. Camp, Langmuir **22**, 5611 (2006).
[34]N. S. S. Mousavi, S. Khapli, and S. Kumar, in 11th ISHMT-ASME Heat and Mass Transfer Conference, IIT Kharagpur, India, 2013.
[35]C. Scherer and A. M. Figueiredo, Braz. J. Phys. **35**, 718–727 (2005).
[36]A. Satoh, R. W. Chantrell, S.-I. Kamiyama, and G. N. Coverdale, J. Colloid Interface Sci. **178**, 620 (1996).
[37]V. S. Mendelev and A. O. Ivanov, Phys. Rev. E **70**, 051502 (2004).
[38]A. Satoh, R. W. Chantrell, S.-I. Kamiyama, and G. N. Coverdale, J. Colloid Interface Sci. **181**, 422 (1996).
[39]J. J. Weis, Mol. Phys. **103**, 7 (2005).
[40]J. Huang, Z. Wang, and C. Holm, Phys. Rev. E: Stat., Nonlinear, Soft Matter Phys. **71**, 061203 (2005).
[41]A. Wiedenmann, U. Keiderling, M. Meissner, D. Wallacher, R. Gähler, R. May, S. Prvost, M. Klokkenburg, B. Ern, and J. Kohlbrecher, Phys. Rev. B: Condens. Matter **77**, 184417 (2008).
[42]J. M. Laskar, J. Philip, and B. Raj, Phys. Rev. E **80**, 041401 (2009).
[43]J. Wu, M. Aslam, and V. P. Dravid, Appl. Phys. Lett. **93**, 082505 (2008).
[44]M. Klokkenburg and B. H. Ern, J. Magn. Magn. Mater. **306**, 85 (2006).
[45]W. X. Fang, Z. H. He, X. Q. Xu, Z. Q. Mao, and H. Shen, EPL (Europhys. Lett.) **77**, 68004 (2007).
[46]T. Cosgrove, *Colloid Science* (John Wiley and Sons, 2010), Chap. 3, p. 46 and Chap. 11, p. 239.
[47]Y. Sahoo, M. Cheon, S. Wang, H. Luo, E. P. Furlani, and P. N. Prasad, J. Phys. Chem. B **108**, 3380 (2004).
[48]M. Klokkenburg, B. H. Ern, J. D. Meeldijk, A. Wiedenmann, A. V. Petukhov, R. P. A. Dullens, and A. P. Philipse, Phys. Rev. Lett. **97**, 185702 (2006).
[49]J. Martin, J. Odinek, and T. Halsey, Phys. Rev. Lett. **69**, 1524 (1992).
[50]T. Halsey and W. Toor, Phys. Rev. Lett. **65**, 2820 (1990).
[51]T. Halsey and W. Toor, J. Stat. Phys. **61**, 1257 (1990).
[52]D. Heinrich, A. R. Goi, A. Smessaert, S. H. L. Klapp, L. M. C. Cerioni, T. M. Osn, D. J. Pusiol, and C. Thomsen, Phys. Rev. Lett. **106**, 208301 (2011).